Ni–W–S nanoparticles in-situ synthesised on Ti mesh for electrocatalytic oxidation of glucose

*Hui Zhao** ✉, *Yuqing Miao**

University of Shanghai for Science and Technology, Shanghai 200093, People's Republic of China
**Hui Zhao and Yuqing Miao contributed equally to this work and can be considered as co-first authors.*
✉ *E-mail: huizhao_usst@126.com*

Published in Micro & Nano Letters; Received on 15th March 2018; Revised on 22nd May 2018; Accepted on 8th June 2018

The Ni–W–S nanoparticles (NPs) were synthesised on Ti mesh through the typical hydrothermal method. The obtained Ti/Ni–W–S was characterised on morphology, composition and electrocatalytic property. It showed good electrocatalytic performance towards glucose oxidation in strong alkali electrolyte, exhibiting the potential application in the field of fuel cell. The excellent electrocatalytic activity of Ni–W–S NPs, the favourable electron transfer between electrode and catalysts, as well as the high conductivity of Ti contributed to its final catalytic performance of Ti/Ni–W–S.

1. Introduction: Glucose is one of the most important monosaccharides in nature [1]. Catalytic oxidation of glucose has been widely applied in analysis and determination in clinic, food, pharmaceutical and environmental areas, which is also primal for the development of glucose-based fuel cells [2–4]. Meanwhile, glucose is the biomass fuel with potentially enormous energy density since its complete conversion to CO_2 transfers 24 electrons [5–8]. The electrochemical oxidation of glucose is a dehydrogenation process and the dissociated hydrogen becomes anode fuel [6, 7, 9]. Compared with methanol and other biomass fuels, glucose is non-toxic, odourless and clean [10, 11].

However, the direct electrocatalytic oxidation of glucose at bare electrode surface is very difficult to achieve due to its sluggish electron transfer dynamics [9, 10, 12, 13]. Inexpensive transition materials have been considered as promising catalysts for oxidation of glucose, owing to recent developments in catalyst preparation technologies with significant improvements in the catalytic activity [4, 14, 15]. On the one hand, the enhanced activity can be obtained by addition of other elements, which helps develop different compounds/nanocomposites or hybridisation with other nanomaterials [14, 16]. On the other hand, the electrocatalytic efficiency is also improved by the electrode substrate on which the catalysts are attached. Usually, metal material is used as carrier which has good electric conductivity, high specific area and long stability [14, 17].

Herein, Ni–W–S nanocatalysts were in-situ synthesised on Ti mesh for electrocatalytic oxidation of glucose. It is expected that such nanocatalysts firmly grow onto the surface of Ti mesh and form steric structure with large specific area, high electrocatalytic activity and excellent stability [14]. The electrocatalysis towards glucose was studied at the obtained Ti/Ni–W–S.

2. Experiments

2.1. Reagents: $Ni(NO_3)_2{\cdot}6H_2O$, $Na_2WO_4{\cdot}2H_2O$ and thioacetamide were purchased from Aladdin Reagent Database Inc. (Shanghai, China). Ti mesh (TA1, mesh number 250, wire diameter 0.16 mm × 0.11 mm, pore diameter 58 μm) was from Anping Ofolan Metal Wire Mesh Manufacture Co. Ltd (Anping, China). The deionised water was used for the preparation of solutions in all the experiments, which was provided by a Milli-Q water purification system (Millipore, Milford, MA).

2.2. In-situ preparation of the Ni–W–S nanoparticles (NPs) on Ti mesh: First, Ti mesh (1 cm × 1 cm × 1 mm) was cleaned through the ultrasonic process in HNO_3, alcohol and deionised water sequentially each for 30 min, and then dried for use.

In a typical procedure, the Ni–W–S NPs were prepared using the following procedure. About 10 ml of 0.5 mM $Ni(NO_3)_2$, 10 ml of 0.5 mM $Na_2WO_4{\cdot}2H_2O$, 20 ml of 2.5 mM thioacetamide, 10 ml of 0.5 mM glucose were mixed under violently stirring within an hour. Then the mixed solution was transferred into a reaction kettle with a piece of Ti mesh inside. After sealed, it was heated to 180°C within 4 h. Then it was maintained at 180°C for 24 h after which it is naturally cooled to room temperature. The Ti mesh with deposited Ni–W–S NPs was washed for several times with deionised water and absolute ethanol to remove remaining reactants. Finally, it was dried at 50°C under vacuum for 6 h to obtain the Ti/Ni–W–S. For comparison, Ni–W–S NPs were also prepared in the similar procedures without Ti mesh.

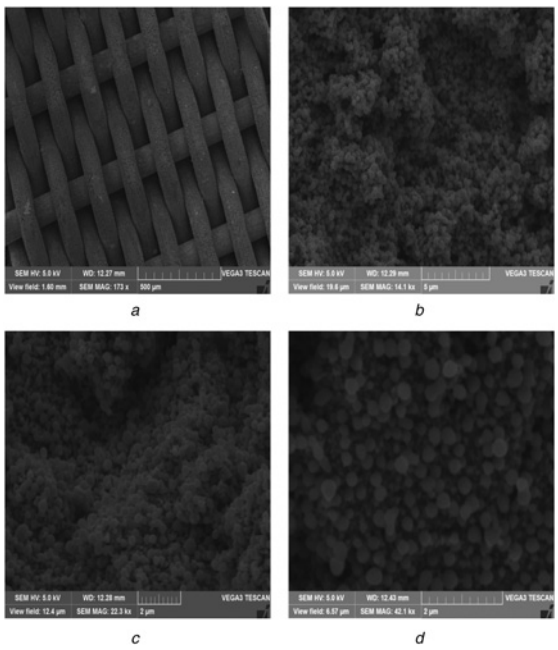

Fig. 1 *SEM images of*
a–d Ni–W–S NPs deposited on the porous Ti mesh

© The Institution of Engineering and Technology 2018

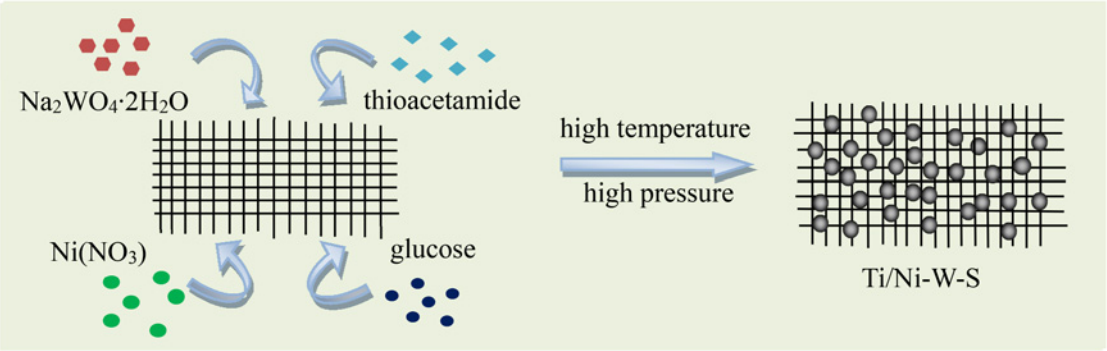

Fig. 2 *Representation of the formation process of the Ti/Ni–W–S*

2.3. Instruments and methods: The morphologies of Ti/Ni–W–S and Ni–W–S were examined by using scanning electron microscopy (SEM, MIRA3 XMU/XMH TESCAN), followed by the determination of the local elemental composition with energy dispersive X-ray spectrometry (EDXS, SYSTEM7, Thermo Fisher). The X-ray diffraction (XRD) pattern was recorded using a D8 Advance X-ray diffractometer (Bruker). The electrochemical properties were measured with a CHI 660D electrochemical workstation (CH Instruments) controlled by computer and software. The Ti/Ni–W–S and Ni–W–S NPs were employed as the working electrode, respectively, a saturated calomel electrode as the reference electrode and a platinum wire as the counter electrode.

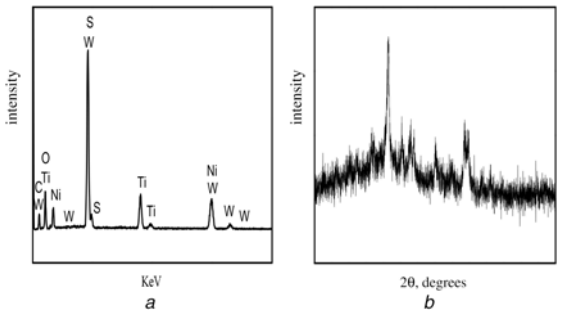

Fig. 3 *EDXS and XRD patterns*
a EDXS of Ni–W–S NPs deposited on the Ti mesh
b XRD patterns of the Ni–W–S

3. Results and discussion: Although glassy carbon electrodes (GCEs) are often used as a support electrode, the direct attachment of the catalysts on GCEs is not stable enough for practical applications. Here, the Ti mesh was employed as supporting electrode to anchor the Ni–W–S nanocatalysts through in-situ synthesis or growth since Ti is high corrosion resistant in strong alkali media and in-situ deposition can lead to the strong adhesion of catalysts [18, 19]. The SEM images of Fig. 1*a* show the reticular structure of Ti mesh with high surface areas so that Ni–W–S NPs can stably attach to its surface and gaps of the Ti mesh. In Figs. 1*b–d*, it is observed that the morphology of deposited Ni–W–S NPs is spherical with the diameter around 340 nm.

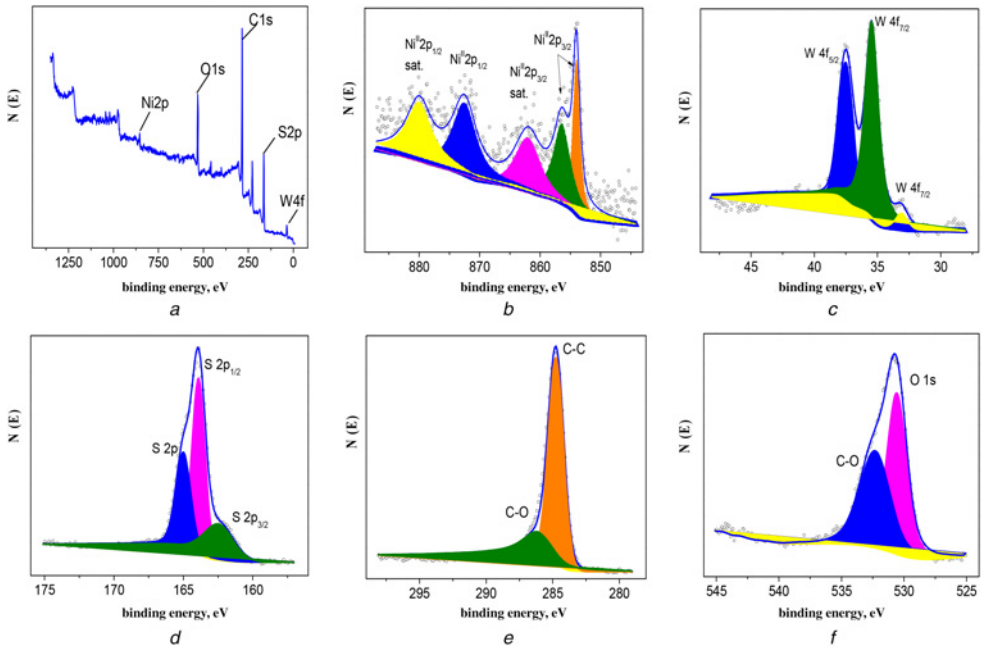

Fig. 4 *Overall and high-resolution XPS spectra*
a Overall XPS spectra of the Ni–W–S NPs deposited on Ti mesh
b–f High-resolution spectra of the Ni–W–S NPs deposited on Ti mesh

© The Institution of Engineering and Technology 2018

doi: 10.1049/mnl.2018.5200

The possible generation mechanism of the Ti/Ni–W–S in hydrothermal reaction is schematically shown in Fig. 2. With the increase of temperature and pressure, there is a nucleation stage of the Ni–W–S NPs on Ti mesh. The carbonation of glucose helps in the formation of microspheres and the doping of Ni, W and S elements.

The EDXS indicates the local elemental composition of the Ti/Ni–W–S. Several peaks corresponding to the elements of Ni, W, S and Ti, which indicates the existence of these elements in samples, are observed in Fig. 3*a*. The atom ratio of Ti:Ni:W:S is about 3.7:5.5:0.04:16.1. The occurrence of C signal is due to the carbonation of glucose. XRD pattern of the Ni–W–S NPs is investigated to analyse its crystal structure in Fig. 3*b*. There are three peaks at 31.6° (004), 53.6° (105) and 54.7° (–242) in Fig. 3*b*, demonstrating the amorphous property of Ni–W–S NPs [20, 21].

Fig. 4 illustrates the surface elemental compositions and electronic state of the Ni–W–S NPs deposited on Ti mesh through X-ray photoelectron spectroscopy (XPS) characterisation. As shown in Fig. 4*a*, the survey of XPS spectrum reveals the presence of Ni, W, S, C and O. These high-resolution XPS spectra of Ni 2p, W 4f, S 2p, C1s and O 1s are shown in Figs. 4*b–f*. The spectrum of Fig. 4*b* shows five peaks, indicating the existence of Ni^{II} in the Ti/Ni–W–S. The peaks at 872.2 eV for Ni^{II} $2p_{1/2}$ and 856.6 eV for Ni^{II} $2p_{3/2}$, accompanied by the satellite peaks at 879.7 eV and 862.5 eV, respectively. A peak at 853.9 eV implies the presence of a different chemical compound of Ni in the divalent state. As shown in Fig. 4*c*, there are peaks at around 37.6 and 35.5 eV due to W $4f_{5/2}$ and W $4f_{7/2}$ of tungsten oxides. In addition, the W $4f_{7/2}$ signal is fitted with peak at 33.1 eV attributed to tungsten disulphide. The S 2p peak in Fig. 4*d* is located at 165.0 eV, corresponding to the organics of sulphur. Besides, there are peaks at around 163.9 and 162.5 eV which are attributed to S $2p_{1/2}$ and S $2p_{3/2}$ of oxides of sulphur. In Fig. 4*e*, two peaks of C 1 s spectrum are observed at 284.8 and 286.3 eV, which are characteristic of C–C and C–O from the carbonation of glucose, respectively. Fig. 4*f* shows the O 1s region from the synthesised Ti/Ni–W–S. The peak at binding energies of 530.6 eV corresponds to the compound of metal oxides like nickel oxide and tungsten trioxide. The other peak of O 1s at 532.3 eV is characteristic of C–O.

To assess the electrocatalytic activity of the Ti/Ni–W–S towards glucose oxidation at anode and the influence of Ni/W ratio on its

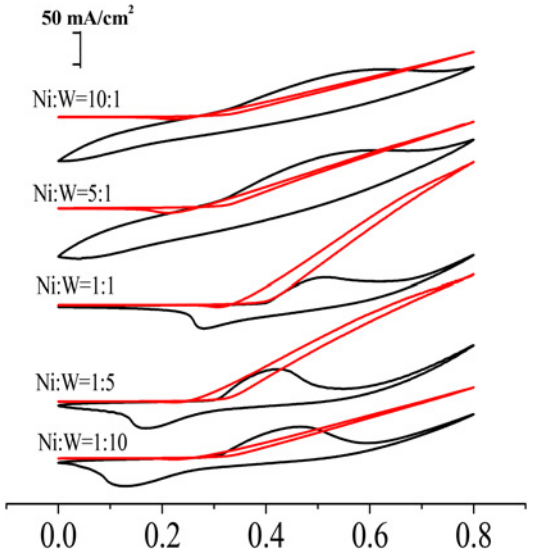

Fig. 5 *Cyclic voltammetry (CV) curves of the Ti/Ni–W–S towards 0.1 M glucose in 0.1 M NaOH. The Ni/W concentration ratios for Ni–W–S synthesis are 10/1, 5/1, 1/1, 1/5 and 1/10, respectively*

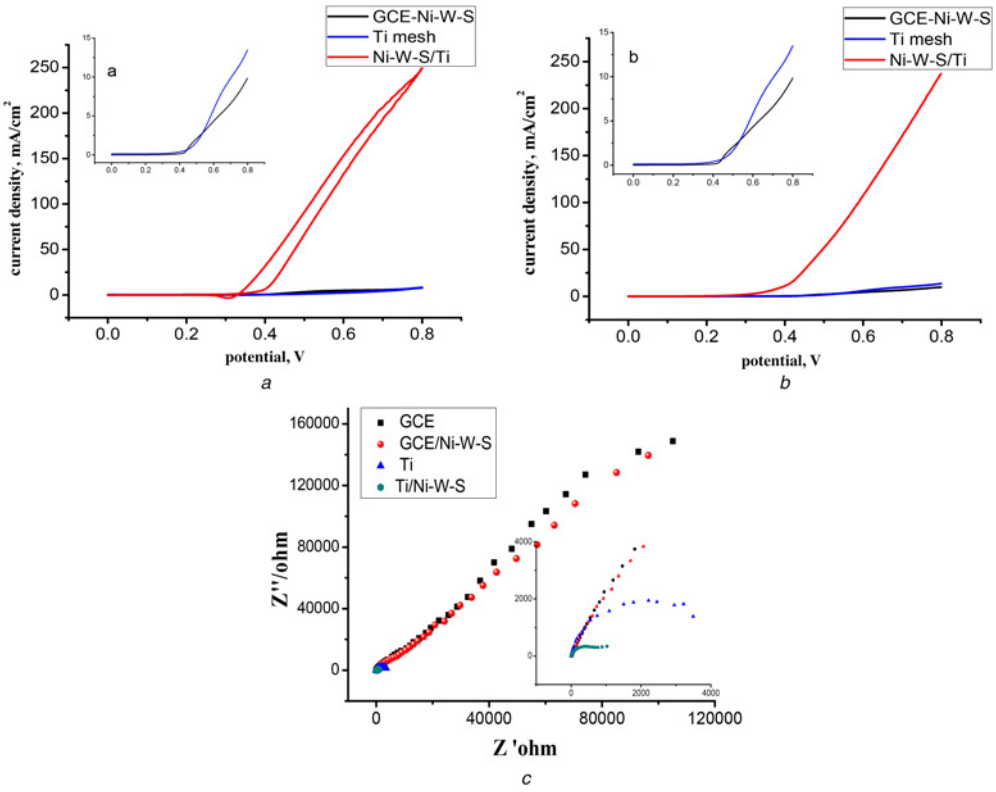

Fig. 6 *Cyclic voltammetric curves, Polarisation curves and Impedance spectra*
a Cyclic voltammetric characterisation of the samples of Ti/Ni–W–S, Ni–W–S and blank Ti mesh in 1 M NaOH with 0.1 M glucose at 0.1 V/s
b Polarisation curves of Ti/Ni–W–S, Ni–W–S and blank Ti mesh in 1 M NaOH with 0.1 M glucose at the scan rate of 0.02 V/s
c Impedance spectra of GCE, GCE-Ni–W–S, blank Ti mesh and Ti/Ni–W–S in 1 M NaOH with 0.1 M glucose

© The Institution of Engineering and Technology 2018

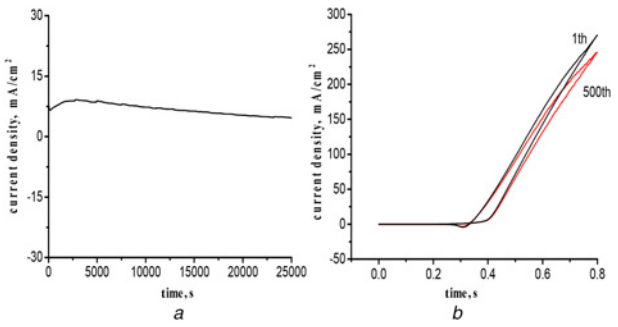

Fig. 7 *Stability test through time-dependent current curve and CV curves*
a Time-dependent current curve of Ti/Ni–W–S under potential 0.5 V for 23,000 s
b First and 500th circles of the CV curve at Ti/Ni–W–S

catalytic performance of glucose, Fig. 5 shows the CV curves of the Ti/Ni–W–S with (red lines) and without (black lines) glucose in 1 M NaOH. The highest electrocatalysis of Ni/W towards glucose was observed with the Ni/W ratio of 1:1. In the presence of glucose, a marked increase in the current with a well-defined peak for glucose oxidation is obtained. This indicates a typical electrocatalytic process and the initiation potential of the glucose oxidation are gained at around 0.4 V. With a significant rise of oxidation current, the vigorous formation of bubbles was observed at both the anode and cathode [22]. Glucose was oxidised electrocatalytically by Ti/Ni–W–S in alkali solution, where the formation of CO_2 and H_2O at anode helps for hydrogen production in cathode.

The electrocatalytic oxidation activity of the Ti/Ni–W–S, Ni–W–S and blank Ti mesh towards glucose in 1 M NaOH was investigated and compared using the CVs in Fig. 6*a*. The Ti/Ni–W–S shows much lower onset overpotential and much higher electrocatalytic oxidation activity than the other two. It means that the combination of Ni–W–S and Ti mesh results in the improved electrocatalytic performance. To further study the catalytic performance of the Ti/Ni–W–S, the polarisation curves presented in Fig. 6*b* were conducted in 1 M NaOH with a scan rate of 0.02 V/s. As observed from the polarisation curves, the onset of oxidation potential appeared at 0.41, 0.47 and 0.43 V with the current density at 236.75, 13.24 and 9.85 mA/cm^2 relative to Ti/Ni–W–S, blank Ti mesh and Ni–W–S, respectively.

Impedance, whose spectroscopy can be used to analyse electron transfer and diffusion characteristics, is an effective tool for studying electrode surface properties and electrochemical catalytic properties. In Fig. 6*c*, the impedance spectroscopy exhibits the representative Nyquist plots of blank GCE, GCE-Ni–W–S, blank Ti mesh and Ti/Ni–W–S. A semicircle can be observed for each of them, which is ascribed to the electron transfer resistance. The Ti/Ni–W–S has the smallest semicircle diameter, indicating the highest efficient electron transportation. Such a low electron transfer resistance may be ascribed to the contact attachment between the Ti mesh and Ni–W–S NPs where the Ti mesh provides high stability and large specific surface area. In addition, no obvious linear part can be found in Nyquist plots of blank Ti mesh and Ti/Ni–W–S in the low-frequency region, which means that the diffusion of ions at catalyst surface is fast enough and no obvious diffusion impedance appears.

Stability is one of the key factors for the long-term operation of electrocatalysts. According to galvanostatic measurements and the current-time test at a constant potential of 0.5 V in Fig. 7*a*, catalysts maintained for 25,000 s in the presence of glucose. It can be seen that the electrocatalytic current of electrocatalytic oxidation is relatively constant and only a slight decrease can be observed. The result shows that the in-situ growth or deposition of Ni–W–S NPs leads to tight contact between catalysts and supporting electrode. At the same time, there is no obvious change in the 1st and 500th circles of the CV curve in Fig. 7*b*.

4. Conclusions: Ni–W–S NPs were in-situ synthesised and organised on Ti mesh in the presence of Ni^{2+}, WO_4^{2-}, thioacetamide and glucose. The carbonation of glucose helps in the formation of microspheres with the doping of Ni, W and S elements. The Ti/Ni–W–S showed high activity for electrocatalytic oxidation of glucose and good stability. The obtained performance can be assigned to good electrocatalysis of Ni–W–S NPs, fast electron transfer of Ti substrate, high specific area of the Ti mesh and Ni–W–S NPs, strong attachment between them, low diffusion hindrance for reactants and products. The Ti/Ni–W–S provides a desirable application of glucose electrolysis for fuel cell.

5 References

[1] Steiner S.M., Duerkop A., Wolfbeis O.S.: 'Optical methods for sensing glucose', *Chem. Soc. Rev.*, 2011, **40**, pp. 4805–4839
[2] Dharuman V., Pillai K.C.: 'Ruo$_2$ electrode surface effects in electrocatalytic oxidation of glucose', *J. Solid State Electrochem.*, 2006, **10**, pp. 967–979
[3] Teymourian H., Salimi A., Firoozi S., *ET AL.*: 'One-pot hydrothermal synthesis of zirconium dioxide nanoparticles decorated reduced graphene oxide composite as high performance electrochemical sensing and biosensing platform', *Electrochim. Acta*, 2014, **143**, pp. 196–206
[4] Zhou K., Zhu Y., Yang X., *ET AL.*: 'Electrocatalytic oxidation of glucose by the glucose oxidase immobilized in graphene-au-nafion biocomposite', *Electroanalysis*, 2010, **22**, pp. 259–264
[5] Simon İ.A., Medeiros N.G., Garcia K.C., *ET AL.*: 'Cuo nanofibers immobilized on paraffin-impregnated graphite electrode and its application in the amperometric detection of glucose', *J. Braz. Chem. Soc.*, 2015, **26**, pp. 121–127
[6] Mamuru S.A., Ozoemena K.I., Fukuda T., *ET AL.*: 'Studies on the heterogeneous electron transport and oxygen reduction reaction at metal (CO, Fe) octabutylsulphonylphthalocyanines supported on multi-walled carbon nanotube modified graphite electrode', *Electrochim. Acta*, 2010, **55**, pp. 6367–6375
[7] Jiang L., Zhang W.: 'A highly sensitive nonenzymatic glucose sensor based on CuO nanoparticles-modified carbon nanotube electrode', *Biosens. Bioelectron.*, 2010, **25**, pp. 1402–1407
[8] Elouarzaki K., Le G.A., Holzinger M., *ET AL.*: 'Electrocatalytic oxidation of glucose by rhodium porphyrin-functionalized MWCNT electrodes: application to a fully molecular catalyst-based glucose/O_2 fuel cell', *J. Am. Chem. Soc.*, 2012, **134**, pp. 14078–14085
[9] Wayne G., Mehmet K., Joshua S., *ET AL.*: 'Biofuel cells for portable power', *Electroanalysis*, 2010, **22**, pp. 727–731
[10] Aoun S.B., Bang G.S., Koga T., *ET AL.*: 'Electrocatalytic oxidation of sugars on silver-upd single crystal gold electrodes in alkaline solutions', *Electrochem. Commun.*, 2003, **5**, pp. 317–320
[11] Azad U.P., Ganesan V.: 'Influence of metal nanoparticles on the electrocatalytic oxidation of glucose by poly(nillteta) modified electrodes', *Electroanalysis*, 2010, **22**, pp. 575–583
[12] Morozan A., Campidelli S., Filoramo A., *ET AL.*: 'Catalytic activity of cobalt and iron phthalocyanines or porphyrins supported on different carbon nanotubes towards oxygen reduction reaction', *Carbon*, 2011, **49**, pp. 4839–4847
[13] Yang Z., Miao Y., Wang T., *ET AL.*: 'The self-adsorption of ni ultrathin layer on glassy carbon surface and their electrocatalysis toward glucose', *J. Electrochem. Soc.*, 2014, **161**, pp. H375–H378
[14] Zhou M., Ouyang R., Li Y., *ET AL.*: '3D microspheres organized from Ni-Mo-S nanoparticles in situ synthesized on porous ti for hydrogen evolution electrocatalysis', *Electrochim. Acta*, 2017, **246**, pp. 9–16
[15] Wang W., Li L., Wu K., *ET AL.*: 'Preparation of Ni-Mo-S catalysts by hydrothermal method and their hydrodeoxygenation properties', *Appl. Catal. A, Gen.*, 2015, **495**, pp. 8–16
[16] Miao Y., Wu J., Zhou S., *ET AL.*: 'Synergistic effect of bimetallic Ag and Ni alloys on each other's electrocatalysis to glucose oxidation', *J. Electrochem. Soc.*, 2013, **160**, pp. B47–B53
[17] Wu H., Lin D., Zhang R., *ET AL.*: 'Facile synthesis and assembly of Ag/NiO nanofibers with high electrical conductivity', *Chem. Mater.*, 2007, **19**, pp. 1895–1897
[18] Xiao M., Cheng R., Hao M., *ET AL.*: 'Onsite substitution synthesis of ultrathin Ni nanofilms loading ultrafine pt nanoparticles for hydrogen evolution', *Acs Appl. Mater. Interfaces*, 2015, **7**, pp. 26101–26107

© The Institution of Engineering and Technology 2018

doi: 10.1049/mnl.2018.5200

[19] Xiao M., Liang X., Li W., *ET AL.*: 'Synthesis of ultrafine Pt/Pd bimetallic nanoparticles and their decoration on mwcnts for hydrogen evolution', *J. Electrochem. Soc.*, 2015, **162**, pp. H415–H418
[20] Xiao M., Zhang Z., Tian Y., *ET AL.*: 'Co–Fe–Se ultrathin nanosheet-fabricated microspheres for efficient electrocatalysis of hydrogen evolution', *J. Appl. Electrochem.*, 2016, **46**, pp. 1–8
[21] Yan Y., Tian Y., Hao M., *ET AL.*: 'Synthesis and characterization of cross-like Ni-Co-P microcomposites', *Mater. Des.*, 2016, **111**, pp. 230–238
[22] Yeo I.H., Johnson D.C.: 'Electrochemical response of small organic molecules at nickel–copper alloy electrodes', *J. Electroanal. Chem.*, 2001, **495**, pp. 110–119

© The Institution of Engineering and Technology 2018